Plasmon-Induced Hot-Carrier Generation differences in Gold and Silver Nanoclusters

Oscar A. Douglas-Gallardo,[†] Matías Berdakin,[‡] Thomas Frauenheim,[¶] and Cristián G. Sánchez[*,§]

†*Departamento de Fisico Química, Facultad de Ciencias Químicas, Universidad de Concepción, Concepción, Chile.*

‡*INFIQC (CONICET—Universidad Nacional de Córdoba), Ciudad Universitaria & Dpto. Química Teórica y Computacional, Facultad de Ciencias Químicas, Universidad Nacional de Córdoba, Ciudad Universitaria, Argentina.*

¶*Bremen Center for Computational Materials Science, Universität Bremen. Bremen, Germany.*

§*CONICET & Facultad de Ciencias Exactas y Naturales, Universidad Nacional de Cuyo, Padre Jorge Contreras 1300, Mendoza, Argentina.*

E-mail: csanchez@mendoza-conicet.gob.ar

Abstract

In the last thirty years, the study of plasmonic properties of noble metal nanostructures has become a very dynamic research area. The design and manipulation of matter in the nanometric scale demand a deep understanding of the underlying physico-chemical processes that operate in this size regimen. Here, a fully atomistic study of the spectroscopic and photodynamic properties of different icosahedral silver and gold nanoclusters have been carried out by using Time-Dependent Density Functional Tight-Binding (TD-DFTB) model. Optical absorption spectra of different icosahedral silver and gold nanoclusters of diameters between 1 and 4 nanometers has been simulated. Furthermore, the energy absorption process have been quantified by means of calculating a fully quantum absorption cross-section using the information contained in the reduced single-electron density matrix. This approach allows us take into account for the quantum confinement effects dominating in this size regime. Likewise, the plasmon-induced hot-carrier generation process under laser illuminations have been explored from a fully dynamical perspective. We have found noticeable differences in the energy absorption mechanisms and the plasmon-induced hot-carrier generation process in both metals which can be explained by their respective electronic structures. These difference can be attributed to the existence of ultra-fast electronic dissipation channels in gold nanoclusters that are absented in silver nanoclusters. To the best of our knowledge, this is the first report that addresses this topic from a real time fully atomistic time-dependent approach.

Introduction

The study of optical properties of matter in the nanometric scale began with Michael Faraday's finding in 1857. Faraday associated the red color of colloidal solutions obtained from his experiments with the existence of finely divided gold particles.[1] Since then the optical properties of noble metal nanostructures (mainly Au and Ag) have always intrigued researchers mainly due to their promising applications in diverse areas.[2–8] Such optical properties have

been intensely studied both experimentally and theoretically in the last decades.[2,3,5,6,8–11] The intense color that colloidal solutions of noble metal nanostructures often exhibit stems from its interaction with electromagnetic radiation which induces collective oscillation of conduction band (CB) electrons, this phenomenon is known as *Localized Surface Plasmon Resonance* (LSPR) or simply *Surface Plasmon Resonance* (SPR). The existence of this phenomenon makes possible that these particles absorb very large amounts of electromagnetic radiation and concentrate it in a very localized space region which is less than its physical dimensions.[6,8] The manipulation of this large amount of localized energy is one of the main challenge within plasmonic field since it would provide a footpath to trigger a great variety of chemical processes by using only absorbed visible light, i.e, it could trigger photochemical process.

The physicochemical parameter that relates the absorbed light power with the amount of incident light is the absorption cross-section (σ_{abs}). This parameter is a measure of the probability of a given species to absorb energy under constant illumination. For noble metal nanoparticles with certain geometries (sphere and prolate and oblate spheroid) and size the σ_{abs} can be calculated from Mie's theory within a classic theoretical framework.[12] However, for very small noble metal nanoparticles (diameter $<$ 5nm) a fully quantum mechanical description should be adopted in the determination of this property due to quantum confinement effects that may play a preponderant role and therefore need to be taken into account. The knowledge of this key parameter, aside from allowing the determination of the total absorbed energy, allows us to estimate the number of particles dispersed in solution since σ_{abs} is directly related with the molar absorptivity coefficient (ϵ) which may be measured spectrophotometrically.[13]

Light absorption in plasmonic nanostructures occurs when the frequency of incident light (ω_{inc}) is in tune with its natural plasmonic oscillation frequency (ω_{SPR}). When the photoexcitation has elapsed, different energy dissipation process may take place, plasmonic excitation can decay through either radiative or non-radiative channels and the relative importance of

this processes depends on the size, shape and chemical nature of particles.[8] For very small particles the main decay mechanism is the non-radiative pathway. Within this, two main process can occur, one is thermal dissipation of the absorbed energy, a mechanism of current interest due to its potential applications in medical thermal treatments, and in the growth of nanostructures.[14] The second mechanism is faster than thermal dissipation and is due to the decoherence of electrons which are part of the plasmon excitation, a process generally known as Landau damping, that results in the generation of hot carriers. Recently, it has been discovered that non-radiative plasmonic decay channels may produce hot-carriers efficiently.[14–16]The plasmon-induced hot-carriers are holes or electrons with energies higher than their corresponding thermal excitation at room temperature. Due to the dramatic enhancement of the absorption cross-section at the maximum of the plasmonic resonance, plasmon-induced hot carrier generation is much more efficient than the direct formation of electron-hole pairs by laser irradiation off the resonance.[17] Plasmon-induced hot-carriers have quickly found applications in diverse areas as photo-catalysis, photo-detection and solar energy harvesting.[17–19]

Despite the potential application of nanostructures in the size range of 1-4 nm, their optical and photo-dynamical properties are still poorly understood due to the complex size-related-quantum and surface-effects that operate at this size scale.[20,21]However, nowadays, the study of these very small systems has turned out experimental and computationally accessible due to advances reached on the experimental and computational methodologies.[21,22]

To explore plasmon-induced hot carrier generation process different approach have been recently employed.[16,23–29] Within more complex theoretical frameworks, it possible to find those based on ab initio many-body calculations, which take into account electron-electron and electron-phonon interactions. Moreover, the size effect and geometry assisted transitions are also included in this kind of calculation and have been considered for exploring the photophysic underlying hot electron generation in finite metallic slabs.[27–29] It is important to stress that these pioneer reports represent the first contributions that assert the importance

of the d-band electrons (i.e. the chemical nature of the metal) on plasmon decay hot carrier generation process at this high level of theory.

Here, a fully atomistic time-dependent study of plasmon-induced hot carriers generation process in icosahedral gold and silver nanoclusters has been explored by using the Time-Dependent Density Functional Tight-Binding (TD-DFTB) approach. Likewise, the optical absorption spectrum and quantum absorption cross-section have been computed for both metals and different sizes.

Computational Method

The electronic structure of the ground state (GS) of all systems here studied has been computed using the self-consistent-charge density-functional-tight-binding (SCC-DFTB) method.[30–32] This method is based on a controlled approximation of Density Functional Theory (DFT) and has been successfully employed to describe the electronic structure and quantum properties of large organic and biological systems.[32,33] Specifically, the DFTB+ package was used,[34] which is an implementation of the SCC-DFTB method to compute the GS Hamiltonian (H_{GS}) and overlap matrix (S) and thus to obtain the initial GS reduced single-electron density matrix (ρ). Hyb-0-2[35,36] and auorg-1-1[37] DFTB parameter sets have been employed in order to obtain the electronic structure for both icosahedral silver and gold nanoclusters, respectively. Here it is important to point out that DFT gives d-band energies with respect to the Fermi level that are lower than other most precise methods.[27–29] As is expected, this failure is inherited by construction in the DFTB parametrization, as can be observed in the original publication of the parameters used in this work for gold[37] where DFT and DFTB bulk gold band structures are compared. To evidentiate the precision of our method Figure S1 the plot bulk densities of states obtained from DFTB. From this results the interband thresholds obtained from our method can be estimated as -2.1 eV and -3.1 eV for gold and silver, respectively. These agree with the ones shown in Figures 4 and 5 implying that there

is no (or very small) effect of the confinement on the band structure. That is a difference of 0.2 eV and -0.4 eV for each metal referred to benchmark calculations employing many body perturbation theory.[29] This differences could be an issue in the case of gold where the interband transitions play a preponderant role in the hot carrier generation (see discussion). Although, is important to point out that the absorption spectra and all the dynamical observables here employed to describe the mechanism behind the hot carrier formation are not a direct emergent of the raw electronic structure, i.e. if the absorption spectrum of gold were computed considering the transition matrix elements constructed with eigenvectors of the unperturbated electronic structure. These result will largely deviate from experimental results. Nevertheless, as is discussed below, the experimental[38] and our theoretical absorption spectra closely agree both qualitatively and quantitatively. The key point here is that spectra calculation takes into account (albeit in a mean field fashion within the approximations implied by the underlying DFT functional) the energy renormalization that comes from the self dynamic evolution that accounts for the Coulomb kernel effects (within said approximation).[39] This energy renormalization corrects the excitation energies, that is the cause behind the close agreement between the experimental and theoretical gold absorption spectra.

The methodology applied to describe the electronic dynamics of the whole system is based on the real-time propagation of the reduced single-electron density matrix (ρ) under the influence of an external time-dependent potential ($\mathrm{V}_{ext}(t)$).

$$\hat{H}(t) = \hat{H}_{GS} + \hat{V}_{ext}(t) = \hat{H}_{GS} - E(t)\hat{\mu} \tag{1}$$

The Hamiltonian (H_{GS}) and overlap (S) matrices obtained from the DFTB+ code are used as initial input to obtain the GS density matrix (ρ_{GS}). The propagation of the reduced single-electron density matrix is calculated through time integration of the Liouville-von Newmann equation of motion in the non-orthogonal basis,

$$\frac{\partial \hat{\rho}}{\partial t} = \frac{1}{-i\hbar}(S^{-1}\hat{H}[\hat{\rho}]\hat{\rho} - \hat{\rho}\hat{H}[\hat{\rho}]S) \tag{2}$$

where S^{-1} is the inverse of the overlap matrix. Dirac delta pulses and sinusoidal time-dependent electric fields have been used as external electric fields to perturb the whole system and obtain different dynamical information such as optical absorption spectra, quantum absorption cross-section, and whole electron dynamic associated with plasmonic excitation for both metals. The method used is fully atomistic in the sense that all species are treated at the atomic level and all properties described stem from the used of a unique model for the electronic structure of the whole system, making no distinction between different species.

Optical absorption spectra for both icosahedral gold and silver nanoclusters have been obtained using as initial perturbation a Dirac delta pulse (E_0=0.001 V/A). Within the linear response regime, when the applied electric field pulse is small, the dipole moment can be written as,

$$\mu(t) = \int_{-\infty}^{\infty} \alpha(t-\tau)E(\tau)d\tau \tag{3}$$

Where α is the time-dependent dynamic polarizability (or linear response function) along the axis over which the external field is applied. In frequency space the dynamic polarizability is related with dipole moment through of the following expression,

$$\alpha(\omega) = \frac{\mu(\omega)}{E_0} \tag{4}$$

The optical absorption spectrum is proportional to the imaginary part of the frequency-dependent dynamic polarizability which can be calculated from the Fourier transform of the time-dependence dipole moment followed by the application of equation 4. In order to broaden the optical absorption obtained from the electron dynamics before carrying out the Fourier transform of time-dependent dipole moment its signal is damped within the simulation window using an exponential function with a time constant of 7 fs. This broadening is a technical necessity for the discrete Fourier transform to produce meaningful results for

a finite (albeit long) dipole signal to reach a negligible value during the simulation window. This procedure broadens each and every spectral line uniformly by 0.033 eV. An arithmetic average of the frequency-dependent dynamic polarizability over the three Cartesian axes has been used to calculate the absorption spectra for all nanoscopic systems here studied.

In order to study the electronic dynamics induced by light absorption processes in both gold and silver nanoclusters, a sinusoidal time-dependent electric field in tune with natural frequency of dipolar SPR band was used as external perturbation ($E(t) = E_0 \sin(\omega_{SPR}^{Au,Ag} t)$). This allows the disclosure of the underlying dynamics that characterizes the excited electronic motion at frequency of plasmonic excitations. Likewise, a deeper understanding of the nature of the excitation can be obtained from the molecular orbital populations dynamics following a laser excitation in tune with the plasmonic excitation. The orbital population can be calculated from the diagonal elements of the time-dependent reduced single-electron density matrix transformed to the GS molecular orbital basis. Also, molecular-orbital-shell populations have been obtained by adding the contributions coming from diagonal elements corresponding to each orbital-shells (s-, p- and d-orbital-shell) for both transitions metals.

Results and discussion

The study of light absorption process in small silver and gold nanoclusters has been addressed from a fully dynamical and atomistic perspective. The ground state electronic properties of all nanoscopic systems here studied have been computed by means of self-consistent-charge density-functional-tight-binding (SCC-DFTB) approach, based on a second order expansion of the exact DFT energy functional around a reference density. On the other hand, the dynamic electronic properties have been calculated through an extension of SCC-DFTB model to the time domain, namely, a time-dependent DFTB scheme. This approach allows us to obtain valuable information about the dynamics triggered by an external perturbation like an external electric field, for more details see Computational Method Section. In this

context, as a first step, the optical absorption spectra for different icosahedral silver and gold nanostructures containing up to 1415 atoms have been obtained. Next, the energy absorption power as function of the nanucluster size and electric field intensity have been explored and quantified by determining the quantum absorption cross-section for metallic nanostructurs containing up to 1415 atoms. And finally, the plasmon-induced hot carriers generation process for both metals have been explored using as example a silver and gold nanoestructure containing 923 metallic atoms.

Optical absorption spectra of icosahedral gold and silver nanoclusters

In order to provide a fully quantum dynamic picture of the photodynamics underlying light absorption process in silver and gold nanoclusters, the first step was the simulation of their optical absorption spectra for different cluster sizes. The structures employed here are nanoclusters with regular icosahedral shape. This choice is based on the fact that for silver nanoclusters it is already known that the icosahedral shape is the most stable geometric isomer in the size regime studied here.[20,40–42] In the case of gold nanoclusters there is evidence that points out to the fact that small distortions from the icosahedral lattice can stabilize the crystalline structure,[43] nevertheless keeping the regular icosahedral structure throughout all our study allow us to perform a meaningful comparison between the results obtained for both metals, focusing only on the electronic origin of the photophysical features here reported.

Figure 1 presents schematic charts with icosahedral nanocluster structures employed for the simulations, where the number of atoms and the diameter of each structure is shown. The left panel of Figure 1 shows the obtained optical absorption spectrum for gold nanoclusters, following the color code depicted in the inset. It can be observed that when the size of the gold nanocluster increases, the dipolar SPR band situated at ~ 2.5 eV is gradually defined from a broad optical absorption band that spreads throughout all the UV-visible

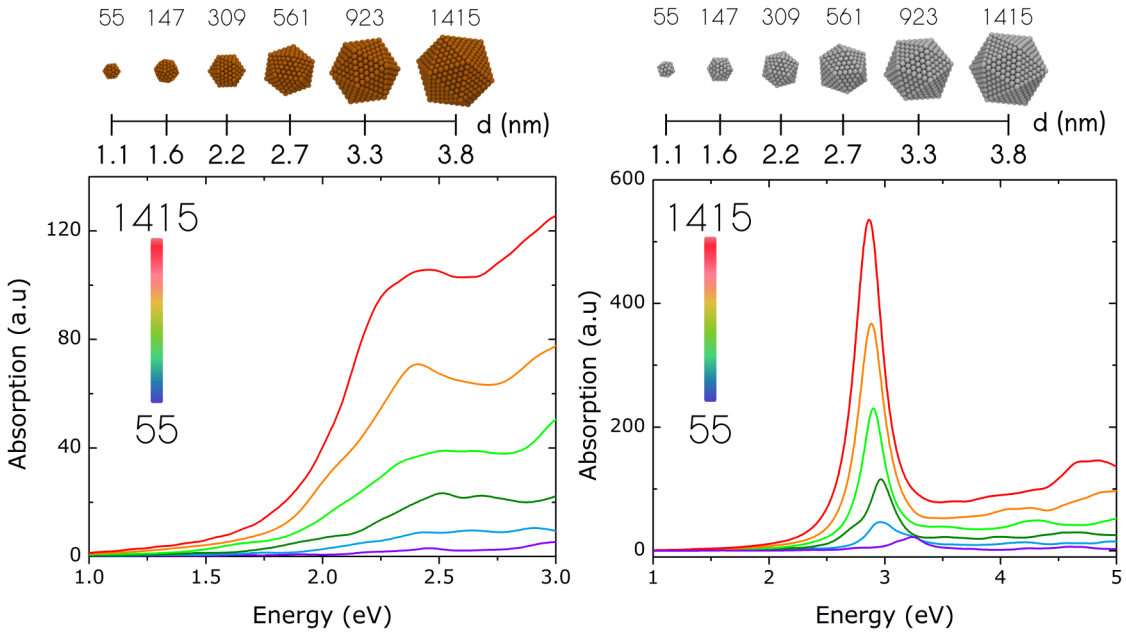

Figure 1: Optical absorption spectra and schematic charts of the structures employed for the simulation, together with the number of atoms and the diameter of each nanocluster, for gold and silver in the left and right panels, respectively.

region and is mainly associated with gold optical inter-band transitions. The dipolar SPR band of the nanocluster with 309 gold atoms is localized at $\sim$ 2.5 eV and is gradually shifted to $\sim$ 2.3 eV (red-shift) for the biggest cluster here studied. This trend is in good agreement with condensed phase experimental results[38,44,45] and those obtained theoretically, at the TD-DFT level[46] and with the Mie theory.[47] This good agreement validates the use of the DFTB electronic structure model presented in the Computational Method section for the study of photphysical properties of gold nanoclusters. In a similar fashion to that presented in Ref 46, the smallest clusters (55 and 147 atoms) present several absorption bands, so the assignment of the dipolar SPR band is rather arbitrary because in this range of size there exist a blurry transition between molecular and plasmonic properties. On the other hand, the simulation of photophysical and photodynamic features of icosahedral silver nanoclusters by means of the theoretical approach here employed, has been extensively described in our previous publications.[48,49] The optical absorption spectra of the silver nonoclusters are presented in the right panel of Figure 1, in this case a pronounced increase of the absorption

intensity and a red-shift of the dipolar SPR band peak position can be clearly observed. This trend is in agreement with experimental[50–53] and theoretically[48] reports. The comparison between the right and left panel of the Figure 1 clearly reproduces two already well-known differences in the optical properties between both metals. First, in the case of the silver nanoclusters, the dipolar SPR band is clearly defined at a smaller cluster size than in the case of gold nanoclusters. Second, the linewidth of SPR band in gold nanoclusters is broader than the linewidth of SPR band in silver nanoclusters. This difference is closely related with the plasmonic excitation lifetime of both metals. In the case of gold nanocluster electronic coherence is lost faster due to intrinsic mechanisms deeply associated to its electronic structure and giving rise to smaller lifetimes. This two well-established spectroscopic features are caused by the energy difference between the d- and sp-band of both metals, a fact that modifies the role of the d-band electrons on the photodymanics of plasmonic relaxation of each metal. This behavior has been extensively discussed in references.[27–29] This will be discussed in terms of electronic dynamics under irradiation conditions in the next section.

A thorough Dynamic Picture of Electronic Energy Absorption Process

Quantum absorption cross-section

As mentioned in the Introduction, the absorption cross-section is a very important property that can be employed in different experimental assays for determining the amount of particles in colloidal solutions and quantifying the amount of energy absorbed by photo-active chemical species. For plasmonic nanoparticles with diameter larger than $\sim$ 10 nm, the absorption cross-section (σ_{abs}) can be obtained from Mie's theory. Nevertheless, when the size of the nanocluster decreases, the calculation of σ_{abs} by means of this classical theory loses accuracy due to the influence of size-dependent quantum confinement and surface scattering effects.[20] Both are very important and should be taken into account for the determination of

σ_{abs}. Here, a fully atomistic quantification of σ_{abs} for silver and gold nanoclusters with size as big as $\sim$ 4 nm has been obtained from a dynamical perspective. In this approach, the quantum and surface effect are suitably accounted within TD-DFTB theoretical framework.

In order to obtain the quantum σ_{abs} both the time-dependent reduced single-electron density matrix ($\rho(t)$) and time-dependent atomic charges (for details see the Computational Methods section) have been employed for calculating the total absorbed energy power (P_{abs}) for each nanostructure from the derivative of the time dependent energy upon constant illumination in resonance with the plasmon within the linear response regime. It is important to stress that P_{abs} is calculated from dynamic information emergent from the electronic dynamics.

For each nanoculster size P_{abs} was calculated under laser irradiation in tune with dipolar SPR excitation energy as a function of the electric field intensity (E_0), which allows us to compute the σ_{abs} by means of Equation 5:[54,55]

$$P_{abs} = \frac{1}{2}\sigma_{abs} n_0 \epsilon_0 c E_0^2 \tag{5}$$

where, n_0, ϵ_0, and c are the relative refractive-index of the medium, permittivity of free space and speed of light in vacuum, respectively. In order to obtain σ_{abs} the quadratic term of Equation 5 was calculated as function of particle size for both noble metals.

Table 1: Quantum absorption cross-section (σ) obtained for gold and silver nanoclusters as function of the cluster size (number of atoms)

Cluster Size	Au(σ/m^2)	Ag(σ/m^2)
147	$\cdots$	$2.3x10^{-19}$
309	$1.0x10^{-19}$	$8.7x10^{-19}$
561	$1.7x10^{-19}$	$1.7x10^{-18}$
923	$3.2x10^{-19}$	$2.2x10^{-18}$
1415	$3.8x10^{-19}$	$4.0x10^{-18}$

The Figure 2 compares the results for the quantum σ_{abs} presented in Table 1 with σ_{abs} obtained from Mie theory for spheres of equivalent volume. These results where calculated both from the bulk dielectric constant of silver and gold and comparative calculations which

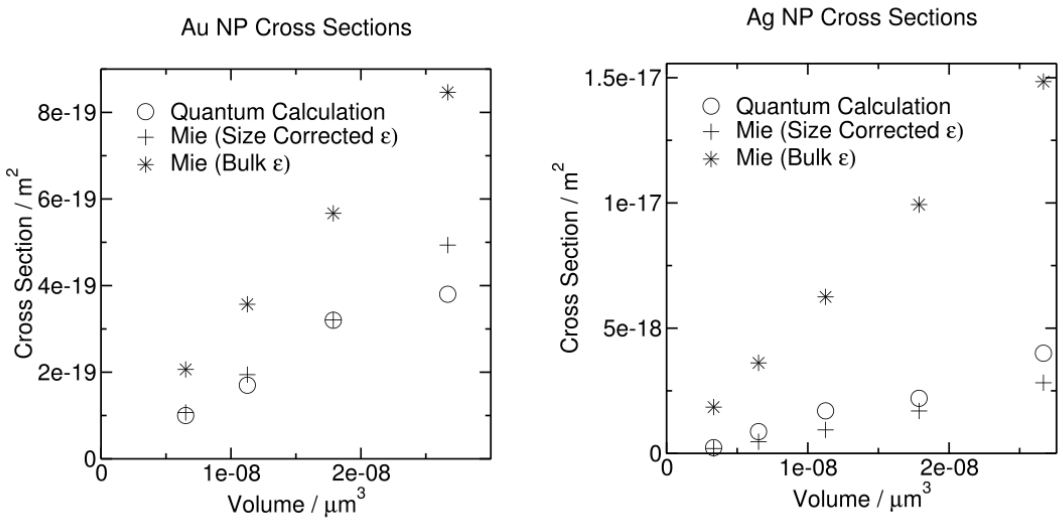

Figure 2: Comparison between absorption cross-section presented in this work with results obtained from Mie theory using the bulk dielectric constant and a size-corrected dielectric constant for each metal.

use corrections of the dielectric function to account for finite size effects.[56,57] The Figure 2 shows the importance of size and quantum effects. Our results are very close to the ones obtained from a size corrected dielectric function. We believe quantum effects are shown in the non-monotonic nature of our results in comparison to the smooth functions of volume that are predicted by Mie theory, directly proportional to volume if the non corrected dielectric function is used. We have reported these non-monotonic features in the lifetime of the plasmonic resonance as a function of size,[58] a fact that has been experimentally reported as well.[59] The comparison in Figure 2 provides striking cross validation of the results presented here and the finite size corrections to the bulk dielectric constant, given that the models used come, on one side from atomistic DFTB calculations and the other from macroscopic electromagnetic theory. These are two very different extremes of physical theory sharing no common parametrization or input between each other.

It is an important point to assess the linearity of the particle response to different incident powers. The P_{abs} and the respective linear fits as a function of E_0 for icosahedral gold and silver nanoclusters with 309 atoms are shown in Figure 3 in orange and gray colors,

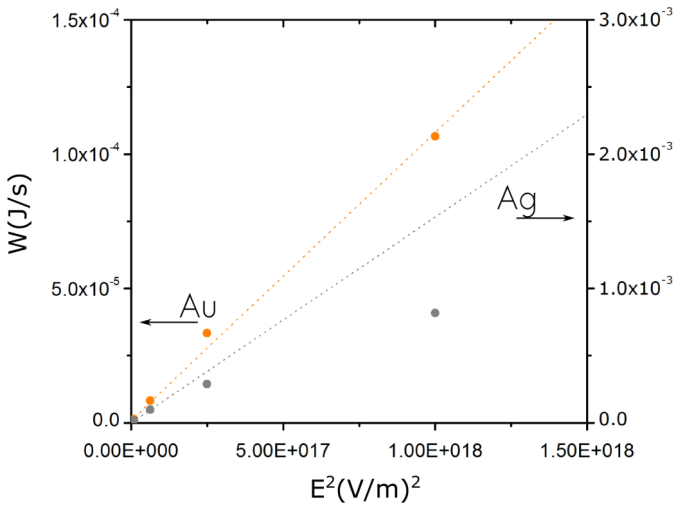

Figure 3: a) Gold (orange) and Silver (gray) 309 nanocluster total absorbed power (P_{abs}) as function of the square of the electric field intensity (dots). Together with the correspondent linear fit employed to calculate σ_{abs} (dashed lines).

respectively. An important aspect of these results can be highlighted. In the case of gold nanoclusters, Figure 3 show that the P_{abs} behaves linearly (with a regression coefficient of 0.999) in the complete range of fields considered. On the contrary, in the case of silver nanoclusters P_{abs} deviates from linearity, and only the smallest field can be accounted within the linear regression. This difference evidences that silver nanoclusters deviate from linear response at smaller fields than gold, and provides a first hint that points out to the existence of non-linear dissipation mechanisms that differentiate the detailed photodynamics triggered after light absorption for both metals.

Plasmon-induced hot-carrier generation

In the following paragraphs, the electronic energy dissipation mechanism in silver and gold nanoclusters will be discussed from a purely dynamic perspective at the time that we disentangle the photodynamics underlying to plasmon-induced hot-carrier generation process for both plasmonic materials.

In order to explore the differences observed in the electronic energy absorption mechanism

between both metals (see Figure 2), a detailed study of photodynamics underlying have been addressed by means of the characterization of electronic structure and the determinations of relevant dynamical properties such as: orbital-shell discriminated population and orbital-shell discriminated absorbed energy. This discussion starts with the results obtained for silver nanoclusters, given that it is already well-established that the plasmonic excitation of silver nanocluster is not perturbed by interband transitions, setting a benchmark on the nature of "intrinsic" plasmonic response. Figure 4 presents the results obtained for the photodynamics of a silver nanocluster with 923 atoms under laser irradiation with a frequency in tune with silver dipolar SPR band (2.885 eV).

Figure 4a shows the orbital-shell resolved absorbed energy ($\epsilon_{abs}^{shell}(t)$), where the s-, p- and d-orbital-shells absorbed energy are depicted in blue, green and red dotted lines, respectively. Furthermore the total energy ($\epsilon_{abs}(t)$) is represented in gray dotted line. In this Figure it can be seen that all orbital-shells contribute to the energy absorption process. At this point, the absorption observed by the d-orbital-shell may sound unexpected but can be rationalized in light of the results presented in Figures 4b and 4c.[48]

Figure 4b shows the change in electronic population ($\rho_{ii}^{Shell}(t)$) for each orbital-shell as consequence of the energy absorption process. On the other hand, Figure 4c shows the evolution of the molecular orbital population, with reference to the ground state, during light irradiation as function of time and the energy of each eigenstate providing a meaningful 2D representation (hereafter called *DynPop* from "dynamical population") of the dynamics underlying the absorption process. In this 2D representation, the color map represents the change of each state population as a function of time, compared with the corresponding population of the unperturbed ground state.

Furthermore in the *DynPop* figure the density of states (DOS) and the projected density of sates (pDOS) are shown. From Figure 4b it can be seen that under light irradiation the s- and d-orbital-shells are depopulated while the p-orbital-shell populates. The sp behavior is expected, provided that the irradiated transition corresponds to the plasmonic excitation.

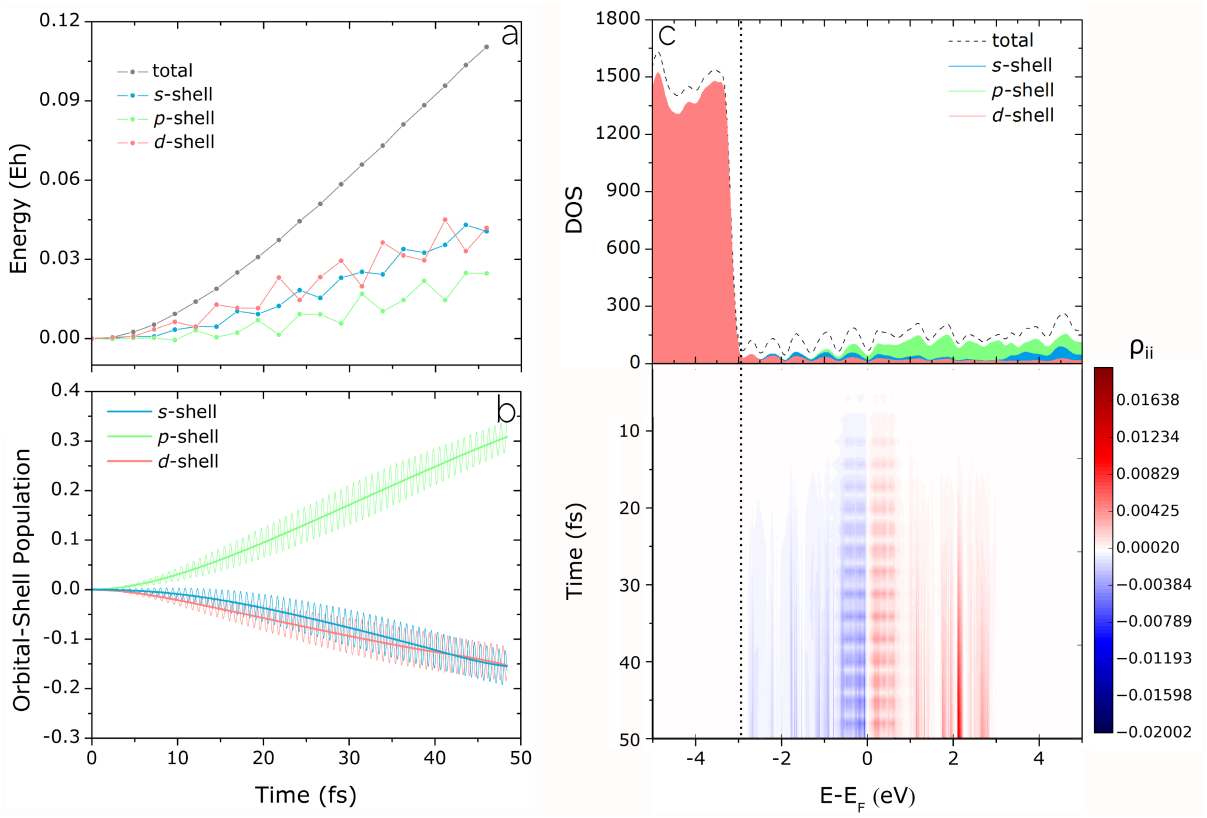

Figure 4: Obtained photodynamics for a silver nanocluster with 923 atoms under laser illumination at 2.885 eV. a) Orbital-shell resolved energy absorption ($\epsilon_{abs}^{shell}(t)$). The energy absorbed by the s, p and d-orbital-shells are depicted in blue, green and red dotted lines, respectively. The total absorbed energy ($\epsilon_{abs}(t)$) is represented in gray dotted lines. b) Orbital-shell population ($\rho_{ii}^{Shell}(t)$) dynamic for s, p and d-orbital-shells in blue, green and red lines, respectively. c) "Dynamical population" (*DynPop*). In this 2D representation, the color map represents the change (increase or decrease) of each state's population as a function of time, compared with the corresponding population of the unperturbed ground state. Furthermore, density of states (DOS) and projected density of sates (pDOS) are shown. The vertical dotted line highlights the start of the d-band.

Concomitantly with this fact Figure 4c shows the population and depopulation of a broad manifold of states near the Fermi level that spans an energy range of ±1 eV, as is expected for the plasmonic response. On the other hand, the energy absorption and depopulation of the d-orbital-shell may mislead to the idea that interband transitions are involved in the surface plasmon excitation of silver nanoclusters. Nevetheless, as was explained in Ref 48 and as is clearly seen in Figure 4c, the d-states involved in the photodynamics do not belong to the bulk of the d-band, but instead arise from the small contibution of localized d-states overlapping in energy with the sp-band. Likewise, the dynamical information contained in Figure 4c allows to recognize the electron-hole pair formation that leads to the population-depopulation of localized states above-below ±1 eV of the Fermi energy. The hot-carrier energy distribution generated is highly symmetric, and as the dynamic evolves involves states with higher energy. It is important to note that the electronic transitions involved in hot-carrier generation process in the case of silver nanoclusters corresponds to intra-band transitions within the sp-band, and begins delayed after the plasmonic excitation starts. The plasmon-induced hot-electron generation process begins only after of 10 fs which is very close to the lifetime associated with silver plasmonic excitation.[48] This is the first time that the plasmon-induced hot-carrier generation process is shown from a fully atomistic and dynamic perspective.

The results obtained for the photodynamics of gold nanoclusters with 923 atoms under laser illumination (2.3 eV) are presented in Figure 5. As it can be seen, the plasmon-induced hot-carrier generation process in gold nanoclusters is very different from that observed for silver nanoclusters in several aspects. As it can be seen in Figure 5a the mechanism depicted by the orbital-shell resolved energy absorption is noticeably different from the one exhibited by silver nanoparticles. Surprisingly, the d-orbital-shell absorbed energy is higher that the energy absorbed by the whole particle. Concurrently, and in agreement with energetic balance, the s- and p-orbital-shell absorbed energy exhibit both negative values and slope. In order to reveal the underlying electronic process that enables this behavior the orbital-shell

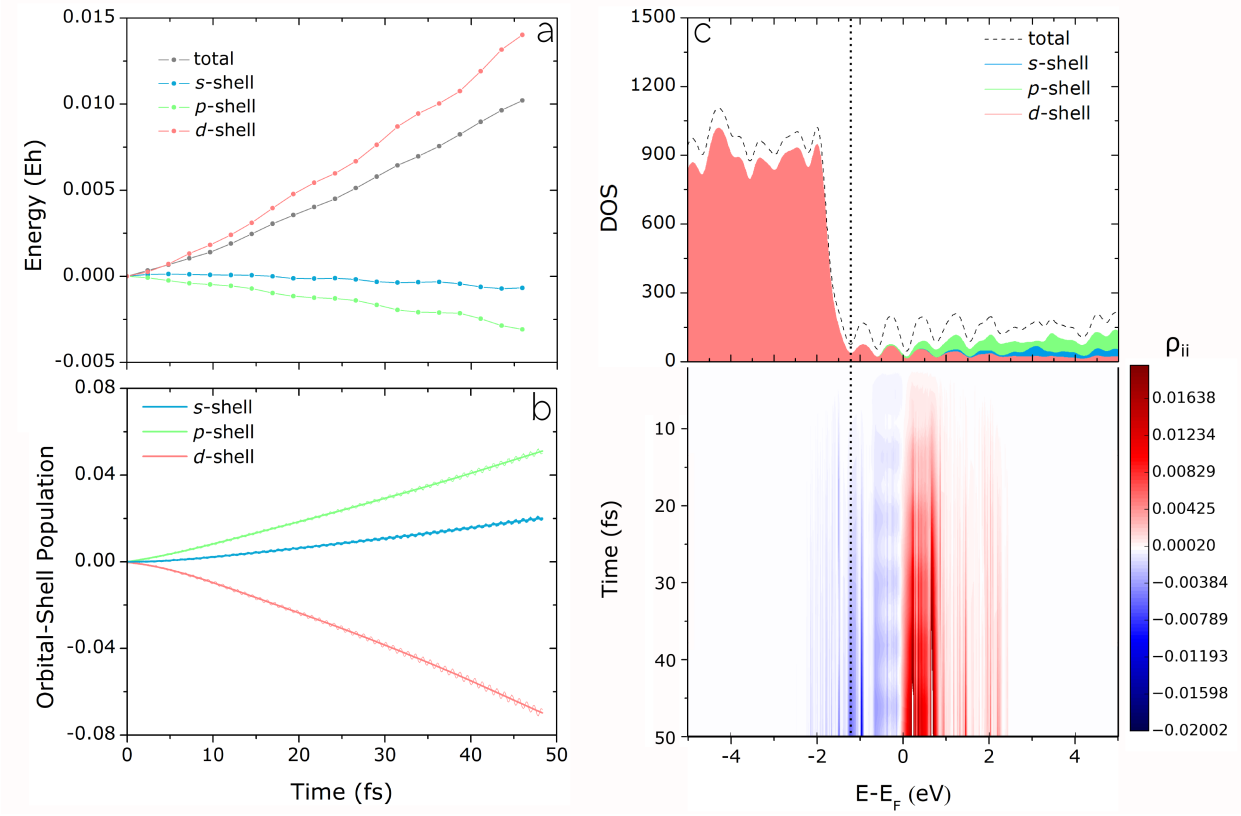

Figure 5: Obtained photodynamics for gold nanocluster with 923 atoms under laser irradiation at 2.34 eV. a) Orbital-shell resolved energy absorption ($\epsilon_{abs}^{shell}(t)$). The absorbed energy by the s-, p- and d-orbital-shells are depicted in blue, green and red dotted lines, respectively. The total absorbed energy ($\epsilon_{abs}(t)$) is represented in gray dotted lines. b) Dynamic orbital-shell population ($\rho_{ii}^{Shell}(t)$) for s-, p- and d-orbital-shells in blue, green and red lines, respectively. c) "Dynamical population" (*DynPop*). In this 2D representation, the color map represents the change (increase or decrease) of each state's population as a function of time, compared with the corresponding population of the unperturbed ground state. Furthermore, density of states (DOS) and projected density of sates (pDOS) are shown. The vertical dotted line highlights the start of the d-band.

population (Figure 5b) and the *PopDy* (Figure 5c) were analyzed. Figure 5b shows that the population of the s-orbital-shell increase with time, pointing out that the rate of s-orbital-shell population is higher that the corresponding depopulation rate, in an opposite fashion to what happens for silver nanoclusters where the depopulation rate leads. Furthermore the *PopDyn* analysis shows, as is expected for the plasmonic excitation, that the states below and above the Fermi energy (± 1 eV) depopulate and populate, respectively. However, in this case the plasmon-induced hot carriers generation process is noticeably different. First, the states involved span both the sp- and d-band. Second, the creation of electron-hole pairs begins concomitantly with plasmonic excitation, which can be explained if we consider the short lifetime that characterizes the gold nanocluster plasmonic excitation. And, finally, the energy distribution of hot-carries shows a slight asymmetry with hot-electrons more energetic that hot-holes. The main difference in photodynamics triggered after light absorption between both metals is the participation of d-electrons in the dynamics, enabled by the close energy proximity between the d- and the sp-band. This modification of the electronic landscape adds a new feature to the dynamic evolution, the sp-excited electrons drain into the d-band. The results can be rationalized as follows, the negative absorbed energy by the s- and p-orbital-shells indicates that for gold nanoclusters an ultra-fast energy dissipation mechanism involved in the hot carriers formation is enhanced, and explains the the origin of the linearity of P_{abs} Vs. E_0^2 in Figure 3a, even for high irradiation fields. This enhancement is originated by the broad energy overlap between the d and sp-band, which provides a high density of d-electrons that acts as a reservoir available to couple with the plasmonic excitation and to dissipate energy. This coupling between the plasmonic response and hot carrier formation drains the SPR absorbed energy through the excitation of d-band electrons to unoccupied states above the Fermi energy, leading to an augmented s-shell population and giving rise to interband hot-carrier creation process. Figure 6 resumes qualitatively the mechanistic differences observed between the hot carrier generation for both metals.

It is important for the reader to note that atoms are fixed in the simulations presented in

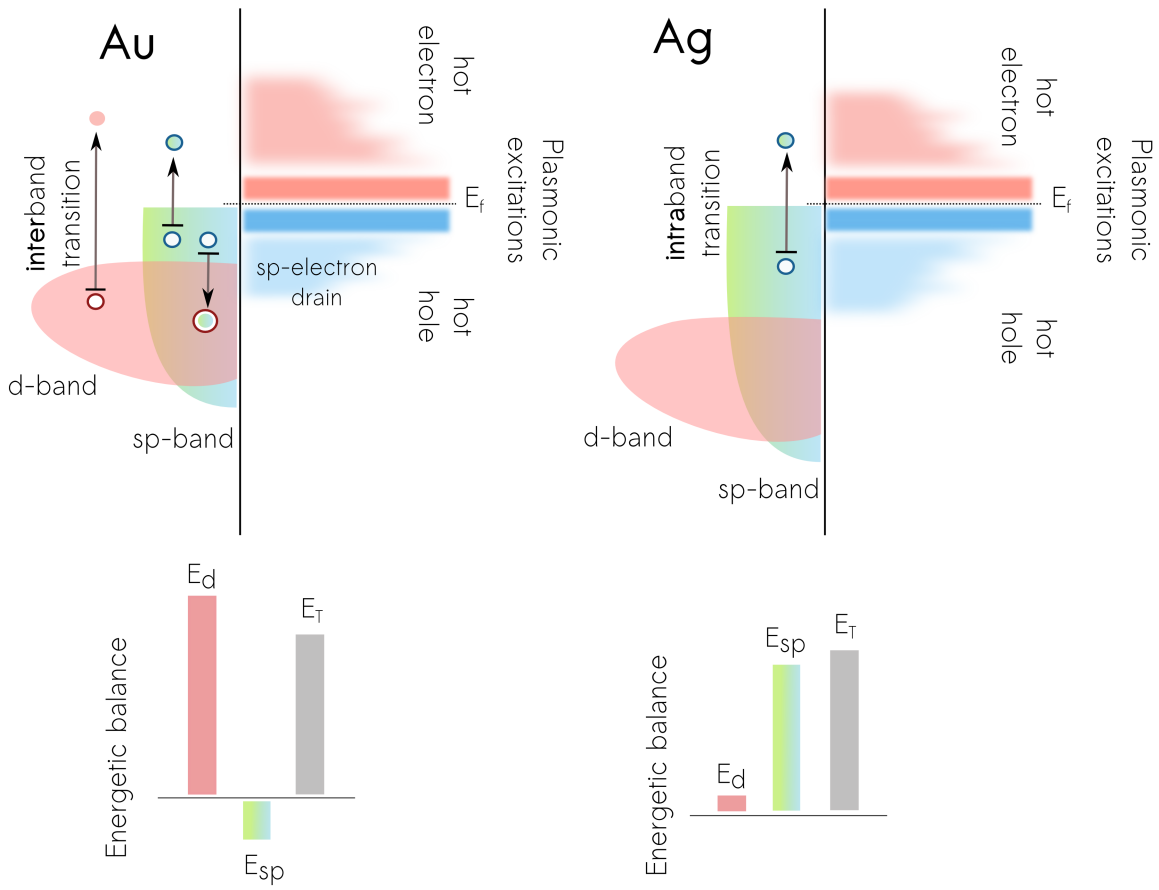

Figure 6: Schematic representation of plasmon-induced hot-electron generation process in gold and silver nanoparticles. The plasmonic excitation is spanned out very near of Fermi level (±1eV) meanwhile electron-hole pairs are progressively generated to higher energy.

the paper, therefore, electron-phonon coupling is not included in the simulation in its present state. Currently, our group is devoted to the development of dynamical methods that include non-adiabatic effects but a non-adiabatic description of the electronic dynamics involved in the hot carrier generation process is far from trivial and currently beyond the scope of the manuscript. With this in mind is important to warn the audience that, particularly in the case of silver nanoparticles, the contribution of phonon-assisted excitation to the initial distribution of hot carriers could be not negligible[27–29] and these are not accounted by our simulation. Nevertheless, the main conclusion of our work involve the impact of d electrons of gold in the dissipation mechanism after the initial excitation, and as it is, this difference in the mechanistic pathway between silver and gold should stand, even if the intraband

transitions in silver are being underestimated by the absence of electron-phonon interaction.

As a final point, it is important to note that the preponderant participation of d-electrons in the hot carrier formation in nano-sized gold particles (and not in silver), agrees with previous publications,[27–29] where the role of d-band electrons was described for metallic bulk and nano-slabs, i.e. this behavior is not modified from the bulk downwards to nanostructure, and highlight the importance of the chemical nature of the metal in the photophysical process. Regarding the mechanistic pathway described above, obtained by means of real time dynamics, we think that provides a complementary picture to the state of the art of the understanding of hot carrier generation process found from many-body approaches.[27–29] How the s-p energy dissipation through the d electrons is modified when the particle size grows to ultimately reach the bulk, is an open question that will allow to set a link between the results presented here and the already established picture from ref.[27–29]

Conclusion

On the basis of a time-dependent DFTB (TD-DFTB) model we have obtained the optical absorption spectra of gold and silver nanocluster for sizes ranging between 1 and 4 nm. Likewise, we have calculated quantum absorption cross-section using the evolution of particle energy upon constant illumination for both noble metal nanoclusters of a range of sizes. Furthermore, we have investigated the electron energy absorption mechanisms and found that gold nanoclusters exhibit electronic energy dissipation channels that are absent in silver nanoclusters. The difference between both mechanistic pathways is associated to the close energy proximity between d-and sp- gold bands in comparison to the silver bands, this difference in the electronic structure landscape allows to the gold plasmonic excitation to couple with the d-band electrons leading to an enhancement of the inter-band hot carrier generation. To the best of our knowledge, this is the first report that addresses this topic from a real time fully atomistic time-dependent approach.

Acknowledgement

The calculations reported where carried out on computational resources from CCAD Universidad Nacional de Córdoba (http://ccad.unc.edu.ar), in particular the Mendieta and Eulogia clusters. CCAD is part of SNCAD-MinCyT, República Argentina. O.A.D.-G. thanks Fondo Nacional de Desarrollo Científico y Tecnológico (Fondecyt) for his postdoctoral fellowship No. 3170029

Supporting Information Available

Bulk silver and gold band structure obtained by means of DFTB simulations.

This material is available free of charge via the Internet at `http://pubs.acs.org/`.

References

(1) Faraday, M. The Bakerian Lecture: Experimental Relations of Gold (and Other Metals) to Light. *Trans. R. Soc. Lond.* **1857**, *147*, 145–181.

(2) Link, S.; El-Sayed, M. A. Shape and size dependence of radiative, non-radiative and photothermal properties of gold nanocrystals. *Int. Rev. Phys. Chem.* **2000**, *19*, 409–453.

(3) Link, S.; El-Sayed, M. A. Optical Properties and Ultrafast Dynamics of Metallic Nanocrystals. *Annu. Rev. Phys. Chem.* **2003**, *54*, 331–366.

(4) Eustis, S.; El-Sayed, M. A. Why gold nanoparticles are more precious than pretty gold: Noble metal surface plasmon resonance and its enhancement of the radiative and nonradiative properties of nanocrystals of different shapes. *Chem. Soc. Rev.* **2006**, *35*, 209–217.

(5) Khlebtsov, N. G.; Dykman, L. A. Optical properties and biomedical applications of plasmonic nanoparticles. *J. Quant. Spectrosc. Radiat. Transf.* **2010**, *111*, 1 – 35.

(6) Coronado, E. A.; Encina, E. R.; Stefani, F. D. Optical properties of metallic nanoparticles: manipulating light, heat and forces at the nanoscale. *Nanoscale* **2011**, *3*, 4042–4059.

(7) Jaque, D.; Martinez Maestro, L.; del Rosal, B.; Haro-Gonzalez, P.; Benayas, A.; Plaza, J. L.; Martin Rodriguez, E.; Garcia Sole, J. Nanoparticles for photothermal therapies. *Nanoscale* **2014**, *6*, 9494–9530.

(8) Hartland, G. V. Optical Studies of Dynamics in Noble Metal Nanostructures. *Chem. Rev.* **2011**, *111*, 3858–3887.

(9) Raza, S.; Kadkhodazadeh, S.; Christensen, T.; Di Vece, M.; Wubs, M.; Mortensen, N. A.; Stenger, N. Multipole plasmons and their disappearance in few-nanometre silver nanoparticles. *Nat. Commun.* **2010**, *6*, 8788.

(10) Alkan, F.; Aikens, C. M. TD-DFT and TD-DFTB Investigation of the Optical Properties and Electronic Structure of Silver Nanorods and Nanorod Dimers. *J. Phys. Chem. C* **2018**, *122*, 23639–23650.

(11) Ranno, L.; Forno, S. D.; Lischner, J. Computational design of bimetallic core-shell nanoparticles for hot-carrier photocatalysis. *NPJ Comput. Mater.* **2018**, *1*, 1–6.

(12) Jain, P. K.; Lee, K. S.; El-Sayed, I. H.; El-Sayed, M. A. Calculated Absorption and Scattering Properties of Gold Nanoparticles of Different Size, Shape, and Composition:Applications in Biological Imaging and Biomedicine. *J. Phys. Chem. B* **2006**, *110*, 7238–7248.

(13) Giblin, J.; Kuno, M. Nanostructure Absorption: A Comparative Study of Nanowire and Colloidal Quantum Dot Absorption Cross Sections. *J. Phys. Chem. Lett.* **2010**, *1*, 3340–3348.

(14) Brongersma, M. L.; Halas, N. J.; Nordlander, P. Plasmon-induced hot carrier science and technology. *Nat. Nanotechnol.* **2015**, *10*, 25–34.

(15) Clavero, C. Plasmon-induced hot-electron generation at nanoparticle/metal-oxide interfaces for photovoltaic and photocatalytic devices. *Nat. Photonics* **2014**, *8*, 95–93.

(16) Zhang, H.; Govorov, A. O. Optical Generation of Hot Plasmonic Carriers in Metal Nanocrystals: The Effects of Shape and Field Enhancement. *J. Phys. Chem. C* **2014**, *118*, 7606–7614.

(17) Mukherjee, S.; Libisch, F.; Large, N.; Neumann, O.; Brown, L. V.; Cheng, J.; Lassiter, B.; Carter, E. A.; Nordlander, P.; Halas, N. Hot Electrons Do the Impossible: Plasmon-Induced Dissociation of H2 on Au. *Nano Lett.* **2013**, *13*, 240–247.

(18) Mukherjee, S.; Zhou, L.; Goodman, A. M.; Large, N.; Ayala-Orozco, C.; Zhang, Y.; Nordlander, P.; Halas, N. J. Hot-Electron-Induced Dissociation of H2 on Gold Nanoparticles Supported on SiO2. *J. Am. Chem. Soc* **2014**, *136*, 64–67, PMID: 24354540.

(19) Du, L.; Furube, A.; Hara, K.; Katoh, R.; Tachiya, M. Ultrafast plasmon induced electron injection mechanism in gold–TiO2 nanoparticle system. *J. Photochem. Photobiol.C* **2013**, *15*, 21 – 30, Next Generation Photochemistry from Asia.

(20) Peng, S.; McMahon, J. M.; Schatz, G. C.; Gray, S. K.; Sun, Y. Reversing the size-dependence of surface plasmon resonances. *Proc. Natl. Acad. Sci. U.S.A.* **2010**, *107*, 14530–14534.

(21) Varnavski, O.; Ramakrishna, G.; Kim, J.; Lee, D.; Goodson, T. Critical Size for the Observation of Quantum Confinement in Optically Excited Gold Clusters. *J. Am. Chem. Soc.* **2010**, *132*, 16–17.

(22) Yau, S. H.; Varnavski, O.; III, T. G. An Ultrafast Look at Au Nanoclusters. *Acc. Chem. Res.* **2013**, *46*, 1506–1516.

(23) Govorov, A. O.; Zhang, H.; Gunko, Y. K. Theory of Photoinjection of Hot Plasmonic Carriers from Metal Nanostructures into Semiconductors and Surface Molecules. *J. Phys. Chem. C* **2013**, *117*, 16616–16631.

(24) Manjavacas, A.; Liu, J. G.; Kulkarni, V.; Nordlander, P. Plasmon-Induced Hot Carriers in Metallic Nanoparticles. *ACS Nano* **2014**, *8*, 7630–7638.

(25) Govorov, A. O.; Zhang, H. Kinetic Density Functional Theory for Plasmonic Nanostructures: Breaking of the Plasmon Peak in the Quantum Regime and Generation of Hot Electrons. *J. Phys. Chem. C* **2015**, *119*, 6181–6194.

(26) Besteiro, L. V.; Govorov, A. O. Amplified Generation of Hot Electrons and Quantum Surface Effects in Nanoparticle Dimers with Plasmonic Hot Spots. *J. Phys. Chem. C* **2016**, *120*, 19329–19339.

(27) Bernardi, M.; Mustafa, J.; Neaton, J. B.; Louie, S. G. Theory and computation of hot carriers generated by surface plasmon polaritons in noble metals. *Nat. Commun.* **2015**, *6*, 7044.

(28) Sundararaman, R.; Narang, P.; Jermyn, A. S.; Goddard III, W. A.; Atwater, H. A. Theoretical predictions for hot-carrier generation from surface plasmon decay. *Nat. Commun.* **2014**, *5*, 5788.

(29) Brown, A. M.; Sundararaman, R.; Narang, P.; Goddard, W. A.; Atwater, H. A. Nonradiative Plasmon Decay and Hot Carrier Dynamics: Effects of Phonons, Surfaces, and Geometry. *ACS Nano* **2016**, *10*, 957–966, PMID: 26654729.

(30) Elstner, M.; Porezag, D.; Jungnickel, G.; Elsner, J.; Haugk, M.; Frauenheim, T.; Suhai, S.; Seifert, G. Self-consistent-charge density-functional tight-binding method for simulations of complex materials properties. *Phys. Rev. B* **1998**, *58*, 7260–7268.

(31) Elstner, M.; Seifert, G. Density functional tight binding. *Philos. Trans. Royal Soc. A* **2014**, *372*.

(32) Christensen, A. S.; Kubař, T.; Cui, Q.; Elstner, M. Semiempirical Quantum Mechanical Methods for Noncovalent Interactions for Chemical and Biochemical Applications. *Chem. Rev.* **2016**, *116*, 5301–5337.

(33) Gaus, M.; Cui, Q.; Elstner, M. Density functional tight binding: application to organic and biological molecules. *Wiley Interdiscip. Rev. Comput. Mol. Sci.* **2014**, *4*, 49–61.

(34) Aradi, B.; Hourahine, B.; Frauenheim, T. DFTB+, a Sparse Matrix-Based Implementation of the DFTB Method. *J. Phys. Chem. A* **2007**, *111*, 5678–5684.

(35) Szuamp, B.; Hajnal, Z.; Frauenheim, T.; González, C.; Ortega, J.; Pérez, R.; Flores, F. Chalcogen passivation of GaAs(1 0 0) surfaces: theoretical study. *Appl. Surf. Sci.* **2003**, *212–213*, 861 – 865.

(36) Szűcs, B.; Hajnal, Z.; Scholz, R.; Sanna, S.; Frauenheim, T. Theoretical study of the adsorption of a {PTCDA} monolayer on S-passivated GaAs(l 0 0). *Appl. Surf. Sci.* **2004**, *234*, 173 – 177.

(37) Fihey, A.; Hettich, C.; Touzeau, J.; Maurel, F.; Perrier, A.; Köhler, C.; Aradi, B.; Frauenheim, T. SCC-DFTB parameters for simulating hybrid gold-thiolates compounds. *J. Comput. Chem.* **2015**, *36*, 2075–2087.

(38) Alvarez, M. M.; Khoury, J. T.; Schaaff, T. G.; Shafigullin, M. N.; Vezmar, I.; Whetten, R. L. Optical Absorption Spectra of Nanocrystal Gold Molecules. *J. Phys. Chem. B* **1997**, *101*, 3706–3712.

(39) Niehaus, T. A.; Heringer, D.; Torralva, B.; Frauenheim, T. Importance of electronic self-consistency in the TDDFT based treatmentof nonadiabatic molecular dynamics.

The European Physical Journal D - Atomic, Molecular, Optical and Plasma Physics **2005**, *35*, 467–477.

(40) Baletto, F.; Mottet, C.; Ferrando, R. Microscopic mechanisms of the growth of metastable silver icosahedra. *Phys. Rev. B* **2001**, *63*, 155408.

(41) Baletto, F.; Mottet, C.; Ferrando, R. Freezing of silver nanodroplets. *Chem. Phys. Lett.* **2002**, *354*, 82 – 87.

(42) Jensen, L. L.; Jensen, L. Atomistic Electrodynamics Model for Optical Properties of Silver Nanoclusters. *J. Phys. Chem. C* **2009**, *113*, 15182–15190.

(43) Li, H.; Li, L.; Pedersen, A.; Gao, Y.; Khetrapal, N.; Jónsson, H.; Zeng, X. C. Magic-Number Gold Nanoclusters with Diameters from 1 to 3.5 nm: Relative Stability and Catalytic Activity for CO Oxidation. *Nano Lett.* **2015**, *15*, 682–688, PMID: 25493586.

(44) Nikhil, R. J.; Latha, G.; Murphy, C. J. Seeding Growth for Size Control of 5-40 nm Diameter Gold Nanoparticles. *Langmuir* **2001**, *17*, 6782–6786.

(45) Kreibig, U.; Zacharias, P. Surface plasma resonances in small spherical silver and gold particles. *Z. Phys.* **1970**, *231*, 128–143.

(46) Iida, K.; Noda, M.; Ishimura, K.; Nobusada, K. First-Principles Computational Visualization of Localized Surface Plasmon Resonance in Gold Nanoclusters. *J. Phys. Chem. A* **2014**, *118*, 11317–11322.

(47) Olmon, R. L.; Slovick, B.; Johnson, T. W.; Shelton, D.; Oh, S.-H.; Boreman, G. D.; Raschke, M. B. Optical dielectric function of gold. *Phys. Rev. B* **2012**, *86*, 235147.

(48) Douglas-Gallardo, O. A.; Berdakin, M.; Sánchez, C. G. Atomistic Insights into Chemical Interface Damping of Surface Plasmon Excitations in Silver Nanoclusters. *J. Phys. Chem. C* **2016**, *120*, 24389–24399.

(49) Bonafé, F. P.; Aradi, B.; Guan, M.; Douglas-Gallardo, O. A.; Lian, C.; Meng, S.; Frauenheim, T.; Sánchez, C. G. Plasmon-driven sub-picosecond breathing of metal nanoparticles. *Nanoscale* **2017**, *9*, 12391–12397.

(50) Scholl, J. A.; Koh, A. L.; Dionne, J. A. Quantum plasmon resonances of individual metallic nanoparticles. *Nature* **2012**, *7290*, 421–427.

(51) Raza, S.; Yan, W.; Stenger, N.; Wubs, M.; Mortensen, N. A. Blueshift of the surface plasmon resonance in silver nanoparticles: substrate effects. *Opt. Express* **2013**, *21*, 27344–27355.

(52) Cottancin, E.; Celep, G.; Lermé, J.; Pellarin, M.; Huntzinger, J. R.; Vialle, J. L.; Broyer, M. Optical Properties of Noble Metal Clusters as a Function of the Size: Comparison between Experiments and a Semi-Quantal Theory. *Theor. Chem. Acc.* **2006**, *116*, 514–523.

(53) Raza, S.; Kadkhodazadeh, S.; Christensen, T.; Di Vece, M.; Wubs, M.; Mortensen, N. A.; Stenger, N. Multipole plasmons and their disappearance in few-nanometre silver nanoparticles. *Nat. Commun.* **2015**, *6*, 8788.

(54) Posthumus, J. *Molecules and Clusters in Intense Laser Fields*; Cambridge University Press, 2001.

(55) He, G.; Liu, S. *Physics of Nonlinear Optics*; World Scientific, 1999.

(56) Genzel, L.; Martin, T. P.; Kreibig, U. Dielectric function and plasma resonances of small metal particles. *Zeitschrift für Physik B Condensed Matter* **1975**, *21*, 339–346.

(57) Coronado, E. A.; Schatz, G. C. Surface plasmon broadening for arbitrary shape nanoparticles: A geometrical probability approach. *The Journal of Chemical Physics* **2003**, *119*, 3926–3934.

(58) Negre, C. F. A.; Sánchez, C. G. Atomistic structure dependence of the collective excitation in metal nanoparticles. *The Journal of Chemical Physics* **2008**, *129*, 034710.

(59) Berciaud, S.; Cognet, L.; Tamarat, P.; Lounis, B. Observation of Intrinsic Size Effects in the Optical Response of Individual Gold Nanoparticles. *Nano Letters* **2005**, *5*, 515–518, PMID: 15755105.

Graphical TOC Entry

Some journals require a graphical entry for the Table of Contents. This should be laid out "print ready" so that the sizing of the text is correct. Inside the `tocentry` environment, the font used is Helvetica 8 pt, as required by *Journal of the American Chemical Society*.
The surrounding frame is 9 cm by 3.5 cm, which is the maximum permitted for *Journal of the American Chemical Society* graphical table of content entries. The box will not resize if the content is too big: instead it will overflow the edge of the box.
This box and the associated title will always be printed on a separate page at the end of the document.